

# Highly Specific Electrochemical Analysis of Cancer Cells using Multi-Nanoparticle Labeling\*\*

Ying Wan, Yi-Ge Zhou, Mahla Poudineh, Tina Saberi Safaei, Reza M. Mohamadi, Edward H. Sargent, and Shana O. Kelley\*

**Abstract:** Circulating tumor cells (CTCs) can be collected noninvasively and provide a wealth of information about tumor phenotype. For this reason, their specific and sensitive detection is of intense interest. Herein, we report a new, chip-based strategy for the automated analysis of cancer cells. The nanoparticle-based, multi-marker approach exploits the direct electrochemical oxidation of metal nanoparticles (MNPs) to report on the presence of specific surface markers. The electrochemical assay allows simultaneous detection of multiple different biomarkers on the surfaces of cancer cells, enabling discrimination between cancer cells and normal blood cells. Through multiplexing, it further enables differentiation among distinct cancer cell types. We showcase the technology by demonstrating the detection of cancer cells spiked into blood samples.

**D**etection and characterization of cancer cells that are shed from tumors into the bloodstream is an important challenge in cancer research. The presence of cancer cells known as circulating tumor cells (CTCs) in the blood of patients is an important hallmark of metastasis,<sup>[1]</sup> a process during which cancer spreads from its original site to secondary organs. Identification and analysis of CTCs can provide a direct and effective method of cancer diagnosis and management.<sup>[2]</sup>

Cancer cells circulating in human blood are exceedingly rare. For this reason it is extremely challenging to quantify these rare cells accurately in the presence of a large excess of nonspecific cells. Numerous techniques, mostly based on fluorescence imaging, have been developed to enumerate cancer cells.<sup>[3]</sup> Although these techniques are widely used, they are expensive, time consuming, and require a high level

of technical skill on the part of the operator. To overcome these challenges, new generations of sensors based on the quartz crystal microbalance (QCM),<sup>[4]</sup> micro-NMR spectroscopy,<sup>[5]</sup> micro-Hall detectors,<sup>[6]</sup> surface-enhanced Raman scattering (SERS),<sup>[7]</sup> electrochemical measurements,<sup>[8]</sup> lateral flow,<sup>[9]</sup> and electrical impedance spectroscopy (EIS)<sup>[10]</sup> have been explored. The detection limits of these methods are in the range of 10 to 8000 cells mL<sup>-1</sup> with most of them above 100 cells mL<sup>-1</sup>, a level of sensitivity that is not high enough for clinical sample analysis. Additionally, most approaches do not identify the cells with sufficient specificity to be applied when a background of nontarget cells are present, and fail to preserve accuracy when challenged with a clinical sample such as blood.

Electrochemical biosensors would—if developed to the point of clinically relevant sensitivity and specificity—represent a particularly attractive solution to cancer cell analysis, as they have previously been shown in related applications to feature high sensitivity, simplicity, rapid response, the capacity for miniaturization, and low cost.<sup>[11]</sup> The electrochemical analysis of specific types of cancer cells has been explored,<sup>[12]</sup> but has not yet been applied successfully in the presence of nontarget cells such as those abundant in a blood sample.

Herein, we report a novel strategy for electrochemical cancer cell identification and multi-marker analysis that relies on the use of a family of metal nanoparticle (MNP) labels that specifically bind to, and enable identification of, target cells. A novel microfabricated chip with multiple gold sensors is produced that captures cells based on an epithelial marker, and then metal nanoparticles modified with antibodies or aptamers for the specific recognition of different biomarkers on the cancer cells are introduced to allow electrochemical detection. Electrochemical scanning allows measurement of the direct oxidation of the MNPs<sup>[13]</sup> and simultaneous detection of different biomarkers on cancer cells is achieved. Using this new strategy, we are able to detect and collect surface marker profiles on as few as two cancer cells per sensor and simultaneously analyze three different surface biomarkers.

The multi-nanoparticle labeling strategy and readout chip are illustrated in Figure 1. To enable multiplexed detection and parallelized measurements, we designed and fabricated a sensor chip containing an array of 11 individual circular 500 μm gold electrodes; ten sensors were used for signal collection and one was used as a control. Each electrode was electrochemically plated with gold, resulting in the formation of a layer of nanoflakes on the electrode (Figure 1A) for maximal capture efficiency.<sup>[14]</sup> The nanostructured gold

[\*] Dr. Y. Wan,<sup>[†]</sup> Dr. Y.-G. Zhou,<sup>[†]</sup> Dr. R. M. Mohamadi, Prof. S. O. Kelley Leslie Dan Faculty of Pharmacy, University of Toronto Toronto, ON (Canada)

M. Poudineh, T. S. Safaei, Prof. E. H. Sargent Department of Electrical and Computer Engineering University of Toronto Toronto, ON (Canada)

Prof. S. O. Kelley Department of Biochemistry, University of Toronto Toronto, ON (Canada) E-mail: shana.kelley@utoronto.ca

[†] These authors contributed equally to this work.

[\*\*] We acknowledge the Canadian Institute of Health Sciences for support of this work with an Emerging Team grant, the Ontario Research Fund for a Research Excellence Grant, and the National Science and Engineering Research Council for a Discovery Grant.



Supporting information for this article is available on the WWW under <http://dx.doi.org/10.1002/anie.201407982>.

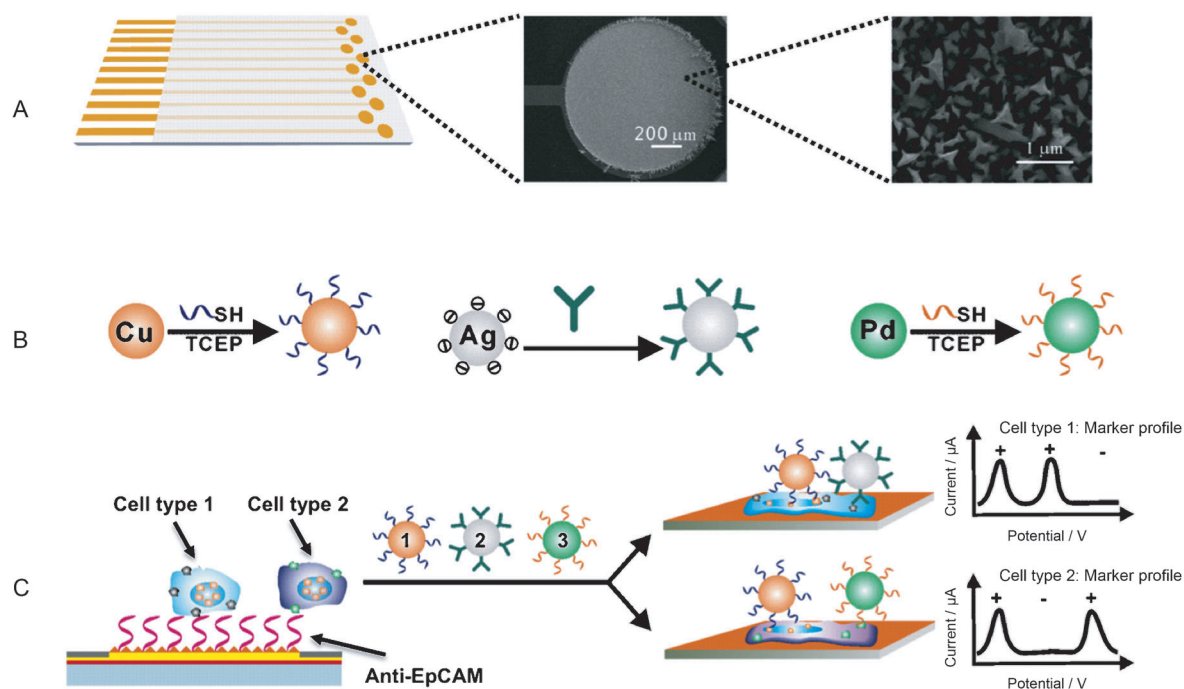


**Figure 1.** Overview of the multi-nanoparticle approach to specific cancer cell detection. A) Chip layout and SEM image of an electrode after plating. Contacts are made with rectangular pads on the surface of the chip, and circular apertures in a layer of SiO<sub>2</sub> serve as working electrodes. SEM scale bars: 200 μm (center), 1 μm (right). B) MNP-based labels are made specific for cell surface markers with DNA aptamers attached using a thiol/metal bond to Cu or Pd nanoparticles or antibodies attached to Ag nanoparticles by electrostatic binding. C) Cancer cells are first captured on an electrode modified with an anti-EpCAM aptamer. A mixture of modified MNPs is introduced and an electrochemical profile is generated using linear-sweep voltammetry (right). TCEP = tris(2-carboxyethyl)phosphine.

electrodes were then coated with a thiolated anti-EpCAM (epithelial cell-adhesion molecule) aptamer for specific capture of epithelial cancer cells. Cancer cells would be captured by the anti-EpCAM aptamer, while nontarget blood cells would not bind at high levels. To ensure minimal amounts of nonspecific binding, mercaptohexanol is used to backfill the EpCAM monolayer.

The electrochemical readout of several markers simultaneously requires redox-active probes with well-separated potentials. We hypothesized that metal nanoparticles (MNPs), made specific to cancer cell surface markers, would serve as good candidates. Based on reported oxidation potentials, we selected Cu, Ag, and Pd as reporters,<sup>[13]</sup> and confirmed that their redox chemistry could be resolved using linear-sweep voltammetry (see Figure S1 in the Supporting Information). We prepared marker-specific Cu and Pd nanoparticles modified with thiol-conjugated aptamers and Ag nanoparticles functionalized with electrostatically bound antibodies (Figure 1B). In a typical assay, these MNP-aptamer/antibody conjugates are incubated with cells captured by EpCAM on the electrode array. Electrochemical scans then oxidize the attached MNPs directly, with different levels of current corresponding to the number of cells present on the sensor (Figure 1C).

To validate the direct MNP strategy as a means of analyzing cancer cells with high levels of sensitivity, the detection of VCaP cells (a cell-based model of human prostate cancer) was carried out using the antibody

Ag-anti-CK18. The titration started with 20 cells suspended in buffer (20 μL), a clinically relevant level of cancer cells.<sup>[15]</sup> Taking into account that a multiplexed chip was used with ten active sensors, two cells are present per sensor. As shown in Figure 2A, an oxidation peak at +450 mV versus Ag/AgCl was detected at this low cell count, and the signal increased as a function of the number of cells introduced to the sensor. The limit of detection was found to be two cells per electrode (Figure 2B). The electrochemical sampling required only a 10 second scan.

The approach was also tested in the presence of blood cells. VCaP cells were spiked into whole blood and detected using Ag-anti-CK18 (Figure 2C). While the overall signal is lower when blood is present, the integrated charge from the Ag oxidation is still detectable in the presence of two cells, and the oxidation peak intensity increases as the cell number goes up. Control experiments carried out in blood without VCaP cells did not yield a significant level of signal, indicating that the approach is highly specific.

Cancer cells in biological samples are significantly outnumbered by normal cells such as white blood cells (WBCs). To discriminate between cancer cells and WBCs, a series of nanoparticle-antibody/aptamer conjugates were selected as electrochemical labels (see Supporting Information) to recognize different markers. Immunofluorescence is the gold standard method used to analyze cancer cells captured from clinical samples, and typically relies on a minimum of three stains:<sup>[16]</sup> 1) a nuclear marker to establish the presence of cells,

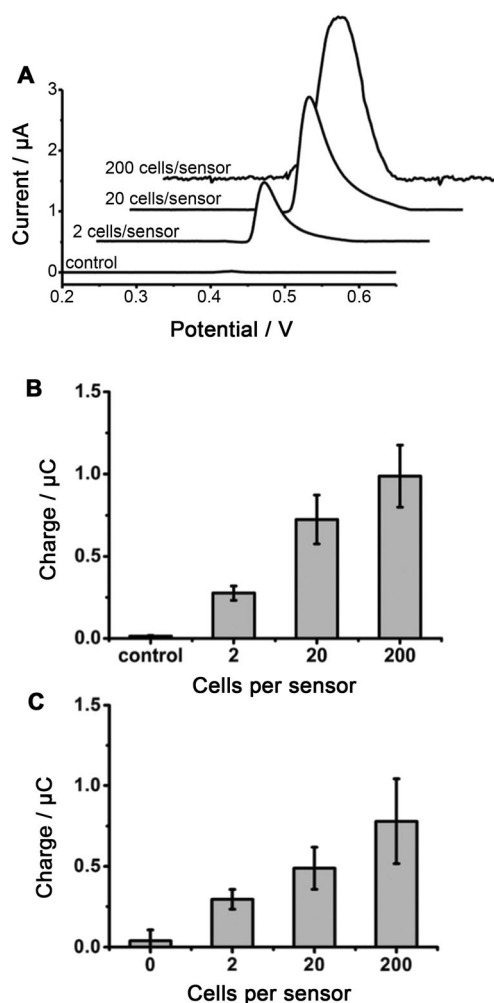


**Figure 2.** Evaluation of electrochemical sensor performance for cancer cell detection using Ag-Anti-CK18. A) Current–potential plots showing the signal intensity in the presence of differing levels of VCaP cells using Ag-Anti-CK18 as a nanoparticle label in PBS. Plots showing limits of detection for VCaP cells in PBS (B) and in blood (C). The control cells used in (A) and (B) are U937 cells present at a level of 2000 cells/sensor. Applied sample volume: 20  $\mu\text{L}$ .

2) an epithelial marker to distinguish the cells as tumor-derived, and 3) a marker specific for WBCs, typically CD45. To replicate this approach using electrochemical monitoring, the following markers were selected: 1) nucleolin, an important nuclear marker that translocates into the outer cell membrane in most cancer cells,<sup>[17]</sup> 2) CK-18, a known epithelial marker, and 3) CD45. Aptamers were obtained for nucleolin and CD45, and the same antibody used above for CK-18 was employed.

The EpCAM-specific sensors were first incubated with VCaP and U937 cells (a WBC model), followed by the application of a mixture of MNPs, including Ag-anti-CK-18 (specific for recognition of VCaP cells), Pd-anti-CD45 (specific for U937 cells), and Cu-anti-nucleolin (a generic marker for both VCaP and U937 cells). As shown in Figure 3 A, two peaks at +300 mV and +640 mV were detected, corresponding to the electrochemical oxidation of Cu and Ag centers from Cu-anti-nucleolin and Ag-anti-CK-18, respectively,

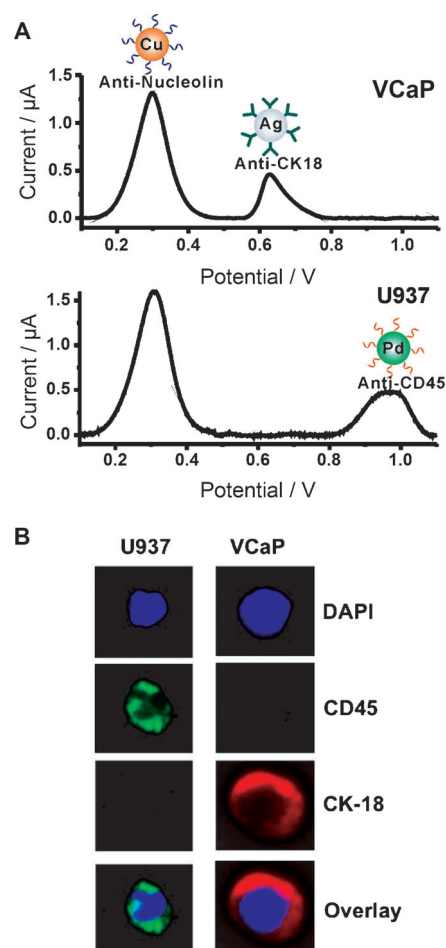


**Figure 3.** Validation of electrochemical identification of cell types using MNP labels. A) Electrochemical analysis of VCaP (top) and U937 (bottom) cells using MNPs Cu-anti-nucleolin, Ag-anti-CK-18, and Pd-anti-CD45. Electrolyte:  $\text{HNO}_3$  (pH 2, 0.01 M). Scan rate: 0.1  $\text{Vs}^{-1}$ . B) Immunofluorescence-based analysis of VCaP and U937 cells for the nuclear marker DAPI (blue) and markers CD45 (green) and CK-18 (red).

while the chip with U937 cells showed two peaks at around +300 mV and +950 mV, corresponding to the oxidation of Cu and Pd centers from Cu-anti-nucleolin and Pd-anti-CD45, respectively. All three peaks ascribed to the direct oxidation of Cu, Ag and Pd centers show a slight shift to positive potentials (compared to the three MNPs directly oxidized on electrode, shown in Figure S1).

A conventional immunostaining experiment was performed with these same cells to illustrate the correspondence of the signals collected with the electrochemical approach (Figure 3 B). In this experiment, the WBC-specific marker anti-CD45 was used, DAPI (4',6-diamidino-2-phenylindole) was employed to stain the nuclei of the cells, and anti-CK was used as an epithelial marker. For VCaP cells, the staining pattern was  $\text{DAPI}^+/\text{CD45}^-/\text{CK}^+$ , which matched the electrochemical analysis. For the U937 cells, the staining pattern was  $\text{DAPI}^+/\text{CD45}^+/\text{CK}^-$ , which also corresponded to what was obtained with electrochemistry. These data illustrate that equivalent results can be obtained using the electrochemical

approach, which provides easily quantifiable results in comparison to immunofluorescence.

Increasingly, cancer therapies are specific to subtypes of cancers, and it is therefore important to analyze cancer cells for specific markers that are associated with tumor phenotype. We selected three different clinically relevant markers, HER2, PSMA, and MUC1. HER2 is found in a subtype of breast cancer that is treatable with targeted therapeutics.<sup>[18]</sup> PSMA is a specific marker found on prostate cancer cells,<sup>[19]</sup> and MUC1 is a marker found on a variety of cancer cells.<sup>[20]</sup> We analyzed three different cell types, MDA-MB-231 cells (derived from MUC1-positive breast cancer), SK-BR-3 cells (derived from HER2-positive breast cancer) and VCaP cells (derived from PSMA-positive prostate cancer), by using a mixture of MNPs targeted towards each marker (Cu-anti-MUC1, Ag-anti-HER2, and Pd-anti-PSMA, respectively). The analysis of the three cell lines shown in Figure 4 A shows

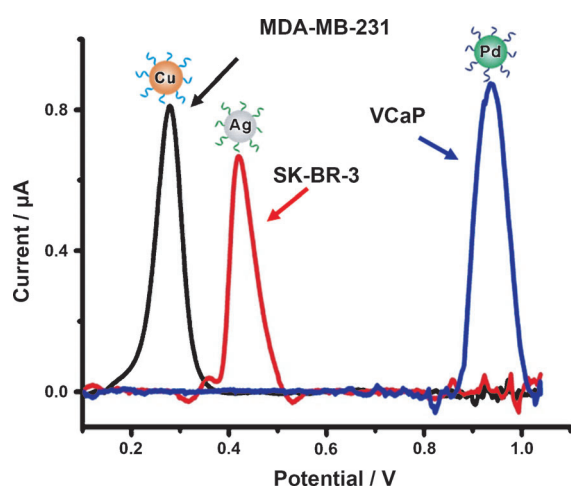


**Figure 4.** Analysis of cancer cell surface markers with mixtures of MNPs. Incubation of VCaP (blue), MDA-MB-231 (black) and SK-BR-3 (red) cells with a mixture of Pd-anti-PSMA, Cu-anti-MUC1, and Ag-anti-HER2 nanoparticles allows the specific detection of surface markers by linear-sweep voltammetry. Electrolyte: HNO<sub>3</sub> (pH 2, 0.01 M). Scan rate: 0.1 Vs<sup>-1</sup>.

three individual oxidation peaks corresponding to the oxidation of Cu-anti-MUC1, Ag-anti-HER2, and Pd-anti-PSMA, respectively, and demonstrates that these markers can be specifically identified. These results also illustrate the versatility of the approach and indicate that it could be used to target any cell type with a unique surface marker.

The sensitivity of the electrochemical assay was further characterized using the three cell lines and three corresponding nanoparticles tested shown in Figure 5. With all three pairs, the signal intensity increased logarithmically with cell number (Figure S4) and the limit of detection was again found to be two cells per sensor. The electrochemical signal for all of the systems tested exhibited a logarithmic dependence on concentration.

This work demonstrates a new multiplexed electrochemical approach that can be applied to the specific detection and characterization of cancer cells. The use of functionalized

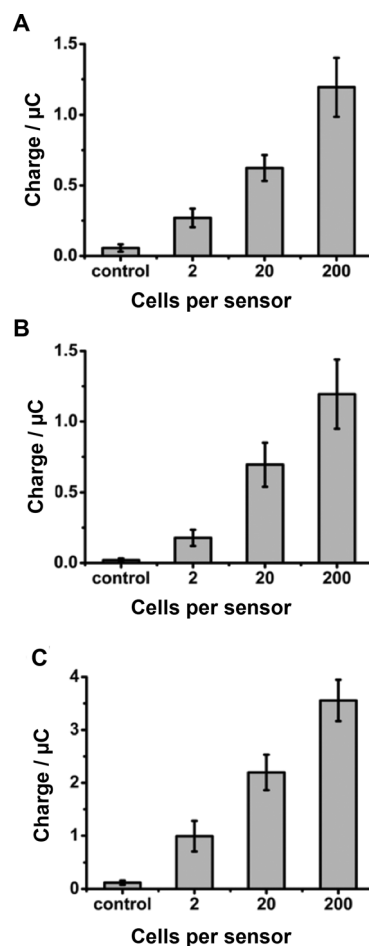


**Figure 5.** Limits of detection for three cell types and corresponding MNPs. A) Analysis of MDA-MB-231 cells using Cu-anti-MUC1 NPs. B) Analysis of SK-BR-3 cells using Ag-anti-HER2 NPs. C) Analysis of VCaP cells using Pd-anti-PSMA NPs. Electrolyte: HNO<sub>3</sub> (pH 2, 0.01 M). Scan rate: 0.1 Vs<sup>-1</sup>. Applied sample volume: 20 µL. Control signals were measured with 200 U937 cells.

metal nanoparticles with well-separated potentials is a critical element of the strategy. While similar results are obtained with this method and using a gold-standard immunostaining approach, the electrochemical analysis method requires less hands-on time and the instrumentation required is much simpler and more cost effective. The approach is highly versatile, as the capture agent can be varied on the electrode, and the recognition agents attached to the metal nanoparticles can also be tailored to detect different cell types. It is noteworthy, however, that the approach relies on the use of known markers previously identified as cancer-cell-specific receptors. Nonetheless, the application of this device to the simultaneous detection and differentiation of different cancer cell types enabled us to demonstrate the discrimination of cancer cells even in the presence of an abundance of white blood cells typically found in patient samples.

Received: August 5, 2014

Revised: September 8, 2014

Published online: October 3, 2014

**Keywords:** antibodies · cancer cells · electrochemistry · metal nanoparticles · surface markers

- 
- [1] J.-M. Hou, M. Krebs, T. Ward, R. Sloane, L. Priest, A. Hughes, G. Clack, M. Ranson, F. Blackhall, C. Dive, *Am. J. Pathol.* **2011**, *178*, 989–996.
- [2] B. Rack, C. Schindlbeck, J. Jückstock, U. Andergassen, P. Hepp, T. Zwingers, T. W. Friedl, R. Lorenz, H. Tesch, P. A. Fasching, *J. Natl. Cancer Inst.* **2014**, *106*, dju066.
- [3] F. Farace, C. Massard, N. Vimond, F. Drusch, N. Jacques, F. Billiot, A. Laplanche, A. Chauchereau, L. Lacroix, D. Planchard, *Br. J. Cancer* **2011**, *105*, 847–853.
- [4] Y. Pan, M. Guo, Z. Nie, Y. Huang, C. Pan, K. Zeng, Y. Zhang, S. Yao, *Biosens. Bioelectron.* **2010**, *25*, 1609–1614.
- [5] A. A. Ghazani, C. M. Castro, R. Gorbatov, H. Lee, R. Weissleder, *Neoplasia* **2012**, *14*, 388-IN382.
- [6] D. Issadore, J. Chung, H. Shao, M. Liong, A. Ghazani, C. Castro, R. Weissleder, H. Lee, *Sci. Transl. Med.* **2012**, *4*, 141ra92.
- [7] a) M. Y. Sha, H. Xu, M. J. Natan, R. Cromer, *J. Am. Chem. Soc.* **2008**, *130*, 17214–17215; b) X. Qian, X.-H. Peng, D. O. Ansari, Q. Yin-Goen, G. Z. Chen, D. M. Shin, L. Yang, A. N. Young, M. D. Wang, S. Nie, *Nat. Biotechnol.* **2008**, *26*, 83–90.
- [8] a) Y. Wu, P. Xue, K. M. Hui, Y. Kang, *ChemElectroChem* **2014**, *1*, 722–727; b) M. Moscovici, A. Bhimji, S. O. Kelley, *Lab Chip* **2013**, *13*, 940–946; c) Y. Zhu, P. Chandra, Y.-B. Shim, *Anal. Chem.* **2013**, *85*, 1058–1064.
- [9] G. Liu, X. Mao, J. A. Phillips, H. Xu, W. Tan, L. Zeng, *Anal. Chem.* **2009**, *81*, 10013–10018.
- [10] Y.-K. Chung, J. Reboud, K. C. Lee, H. M. Lim, P. Y. Lim, K. Y. Wang, K. C. Tang, H. Ji, Y. Chen, *Biosens. Bioelectron.* **2011**, *26*, 2520–2526.
- [11] D. W. Kimmel, G. LeBlanc, M. Meschievitz, D. E. Cliffler, *Anal. Chem.* **2012**, *84*, 685–707.
- [12] a) X. Chen, Y. Wang, Y. Zhang, Z. Chen, Y. Liu, Z. Li, J. Li, *Anal. Chem.* **2014**, *86*, 4278–4286; b) M. Maltez-da Costa, A. de La Escosura-Muñiz, C. Nogués, L. Barrios, E. Ibáñez, A. Merkoçi, *Small* **2012**, *8*, 3605–3612.
- [13] Y. G. Zhou, N. V. Rees, R. G. Compton, *Angew. Chem. Int. Ed.* **2011**, *50*, 4219–4221; *Angew. Chem.* **2011**, *123*, 4305–4307.
- [14] a) L. Soleymani, Z. Fang, E. H. Sargent, S. O. Kelley, *Nat. Nanotechnol.* **2009**, *4*, 844–848; b) W. Chen, S. Weng, F. Zhang, S. Allen, X. Li, L. Bao, R. H. Lam, J. A. Macoska, S. D. Merajver, J. Fu, *ACS Nano* **2013**, *7*, 566–575.
- [15] C. Alix-Panabières, H. Schwarzenbach, K. Pantel, *Annu. Rev. Med.* **2012**, *63*, 199–215.
- [16] K. Pantel, C. Alix-Panabieres, *Trends Mol. Med.* **2010**, *16*, 398–406.
- [17] D. H. M. Dam, J. H. Lee, P. N. Sisco, D. T. Co, M. Zhang, M. R. Wasielewski, T. W. Odom, *ACS Nano* **2012**, *6*, 3318–3326.
- [18] C. A. Hudis, *N. Engl. J. Med.* **2007**, *357*, 39–51.
- [19] S. Papa, N. Emami-Shahri, Z. Liu, U. Petrausch, G. Mullen, J. Spicer, J. Maher, *Lancet* **2014**, *383*, S77.
- [20] J. Taylor-Papadimitriou, J. Burchell, D. W. Miles, M. Dalziel, *Biochim. Biophys. Acta Mol. Basis Dis.* **1999**, *1455*, 301–313.
-